sustainability

MDPI

Article

Influence of pH and Temperature on Struvite Purity and Recovery from Anaerobic Digestate

Carolina González-Morales [1,2,*], Belén Fernández [3], Francisco J. Molina [1], Darío Naranjo-Fernández [1], Adriana Matamoros-Veloza [4] and Miller Alonso Camargo-Valero [2,*]

1 Grupo GAIA, Escuela Ambiental, Facultad de Ingenieria, Universidad de Antioquia, Medellin 050010, Colombia; francisco.molina@udea.edu.co (F.J.M.); dario.naranjo@udea.edu.co (D.N.-F.)
2 BioResource Systems Research Group, School of Civil Engineering, University of Leeds, Leeds LS2 9JT, UK
3 IRTA–GIRO Program, Institute of Agrifood Research and Technology, 08001 Barcelona, Spain; belen.fernandez@irta.cat
4 Institute of Functional Surfaces, School of Mechanical Engineering, University of Leeds, Leeds LS2 9JT, UK; A.MatamorosVeloza@leeds.ac.uk
* Correspondence: carolina.gonzalezm@udea.edu.co (C.G.-M.); M.A.Camargo-Valero@leeds.ac.uk (M.A.C.-V.); Tel.: +44-(0)-113-3431580 (M.A.C.-V.)

Abstract: The precipitation of struvite ($MgNH_4PO_4.6H_2O$) from wastewater streams simultaneosuly recovers nitrogen (N) and phosphorus (P) for reuse as fertilisers. Struvite crystallisation is controlled by pH, saturation index, temperature and other ions in the solution (e.g., Ca^{2+}, Mg^{2+} and $CO_3{}^{2-}$). This work studies the effect of pH and temperature on phosphorus and nitrogen removal via struvite precipitation and the quality of the resulting precipitate product (i.e., crystal size, morphology and purity). Struvite was precipitated in batch reactors from the supernatant produced during anaerobic sludge dewatering at a wastewater treatment works, under controlled pH (8, 9 and 10) and temperature (25, 33 and 40 °C) conditions. The optimal P removal as struvite, reduction of the co-precipitation with Ca and the increase in particle size of the struvite precipitates were determined. The results showed that temperatures of 33 °C and 40 °C are not recommended for struvite precipitation—i.e., at 33 °C the purity is lower, and at 40 °C the ammonia losses are induced by volatilisation. At all pH-tests, the P removal efficiency was >93%, but the highest phosphate content and purity as struvite were obtained at a pH of 9.0. The optimum pH and temperature for the formation of large crystals (84 µm) and a high purity (>70%) of the struvite precipitates were 9 and 25 °C, respectively.

Keywords: centrate; nutrient recovery; saturation index; struvite crystallisation; sustainable sanitation

Citation: González-Morales, C.; Fernández, B.; Molina, F.J.; Naranjo-Fernández, D.; Matamoros-Veloza, A.; Camargo-Valero, M.A. Influence of pH and Temperature on Struvite Purity and Recovery from Anaerobic Digestate. *Sustainability* **2021**, *13*, 10730. https://doi.org/10.3390/su131910730

Academic Editor: Andreas N. Angelakis

Received: 15 July 2021
Accepted: 13 September 2021
Published: 27 September 2021

1. Introduction

Phosphorus (P) is considered a non-renewable resource and is irreplaceable in crop and livestock production; intensive production of P fertilisers from phosphoric rocks is contributing to the fast depletion of commercial and affordable phosphorus global reserves [1]. Therefore, the recovery of P from waste streams such as sewage and sewage sludge at wastewater treatment works (WWTWs) would provide a more sustainable option for P fertiliser supply and would help to reduce the impacts of P shortages in the future. The reuse of wastewater and the recycling of nutrients (nitrogen and phosphorus) to support crop production has been a common practice for decades, with recent global estimates reporting as much as 3.5 billion m^3/year of untreated, partially treated or partially diluted wastewater being used to irrigate at least 20 million hectares across 50 countries (10% of the total irrigated land, which is 17% of the total arable land) [2]. Despite the existence of guidelines for the safe reuse of wastewater in agriculture [3], the presence of emerging pollutants and sometimes the impracticality of irrigating crops located far from wastewater treatment facilities, demands alternative options that allow for the recovery

of valuable nutrients such as P, while making use of the existing fertiliser supply and distribution chains.

The recovery of P in the form of struvite ($MgNH_4PO_4.6H_2O$) is often achieved through P-rich waste streams such as sludge dewatering liquor and digester supernatant at WWTWs [4]. Struvite is a white crystalline mineral composed of magnesium, ammonium, and phosphate (MAP) in an equal molar ratio (1:1:1). This mineral can potentially be used as an eco-fertiliser, competing against traditional fertilisers only if its crystallisation process is well controlled. Struvite is considered a slow-release fertiliser ideal for agriculture, as it reduces nutrient run-off and the subsequent impact on water bodies [5].

Wastewaters with a high concentration of N and P are a suitable source for nutrient recovery via struvite precipitation. Recently, struvite has been recovered from different types of wastewaters, such as swine wastewater, anaerobic digester supernatant, industrial wastewater, agro-industrial wastes and anaerobic digester effluents [6]. During the anaerobic digestion of the sewage sludge in WWTWs, NH_4^+-N, PO_4^{3-}-P and other nutrients (Mg^{2+}, K^+, Ca^{2+}) are released from the digested solid into the liquid phase. This makes the supernatant from digested sludge dewatering (centrate) a great source for the potential recovery of nutrients via struvite precipitation, particularly in WWTWs with an enhanced biological phosphate removal (EBPR) [7].

Struvite precipitation is controlled by the pH, saturation index, temperature and the presence of other ions such as calcium (Ca^{2+}), magnesium (Mg^{2+}) and carbonates (CO_3^{2-}) that can inhibit or reduce struvite formation, depending on their relative concentrations [8]. Previously, the effect of the pH was investigated as a function of the struvite recovery efficiency; it was concluded that an optimum pH range is between 7 and 11 for struvite crystallisation [8,9] as well as P and N removal and recovery [6], since the struvite solubility reaches a minimum solubility at pH values between 9.0 and 10.7 [10,11]. Besides this, the pH has a significant effect on the growth rate and size of struvite crystals. High pH values cause an increase in supersaturation and a subsequent increase in the struvite growth rate [12]. Other works have reported that high pH values increase the density of the nuclei population, yielding smaller, heterogeneous crystals [6].

However, the concentration of Mg^{2+}, NH_4^+ and PO_4^{3-} ions also depends on the pH: a high pH promotes the precipitation of magnesium and calcium phosphate, lowering the quality of the struvite and making it a less-valuable product [6,13]. The calcium interference in struvite precipitation has been extensively investigated with inconclusive results. It has been suggested that the Ca^{2+} could interfere in the crystallisation process of the struvite by promoting the formation of calcium phosphate [14], but it has also been suggested that such an interference depends on the alkalinity or molar ratios of the N:P and Ca:Mg [14,15]. Other works have reported an increase in the kinetics rate for the formation of struvite when Ca^{2+} is present [16]. It was also reported that, although the fast Ca-phosphate precipitation can be dominant at the beginning of the reaction, a high thermodynamic driving force of the struvite precipitation could drive the re-dissolution of the Ca-ions from the Ca-phosphate compounds, favouring a higher purity crystallisation of the struvite [17]. Other investigations have confirmed the presence of $CaCO_3$ and $Ca_3(PO_4)_3$ together with the struvite; however, the presence of Mg^{2+}, PO_4^{3-} and dissolved organic compounds can decrease the precipitation rate of the $CaCO_3$ [14,18].

In addition, it is well known that the concentration of Mg^{2+}, NH_4^+ and PO_4^{3-} ions is pH-dependent, which in turn controls the struvite solubility which decreases as the pH increases, reaching a minimum solubility at pH values between 9.0 and 10.7 [10,11]. Thus, various research works have demonstrated that the increase in pH enhances the P and N removal and recovery [6]. Although a high pH value has been reported to increase the P recovery efficiency, it also promotes the co-precipitation of magnesium and calcium phosphates together with the struvite, making it a less-valuable product [6,13]. No consensus has been reached regarding the optimal pH value required to obtain both the high removal efficiency of P and N from the nutrient rich wastewaters and a high

quality struvite as a final product [9,19]; however, such differences likely lie in the different compositions of the wastewaters [20].

Temperature has a relatively less significant effect on struvite precipitation than the pH, ionic composition or ionic saturation conditions [21]; however, the temperature strongly influences the growth rate and the efficiency of phosphate removal [22]. Struvite solubility and ionic speciation are sensitive to temperature [8,23]. It is known that the solubility of the struvite increases with temperature, reaching a specific value after which the solubility decreases. However, there is disagreement surrounding what that value is; temperature values of 30, 35 and 50 °C have been reported in the literature [24–26].

Besides the temperature, pH and the presence of other ions, the supersaturation of the struvite is an inclusive parameter that should be considered in the operation of struvite precipitation processes because it considers the impact of several factors (struvite constituent ions, ionic strength, pH and temperature) [27] affecting the morphology and particle size that are important for the potential use of struvite as a fertiliser.

Given the current disagreement in the literature regarding the process conditions leading to a high nutrient removal efficiency and high-quality struvite precipitation, this work evaluates the influence of the pH, temperature, and SI on struvite precipitation (quantity and quality) and on P and N removal using the centrate from the dewatering of digested sewage sludge in a real complex medium, as the initial material for struvite formation. The quality of the precipitate formed was assessed by X-ray diffraction (XRD), whilst the morphology and size of the struvite crystals were identified and quantified using scanning electron microscopy (SEM).

Then, the optimal pH and temperature conditions favouring the maximum efficiency of struvite recovery were evaluated in terms of an ion mass balance ensuring the optimal N: Mg: P: Ca molar ratios.

2. Materials and Methods

2.1. Sample Collection and Description of the Full-Scale Wastewater Treatment Works

The Yorkshire Water's Esholt WWTW (Bradford, West Yorkshire, UK) treats 280,000 m^3/d of domestic and industrial wastewater from municipalities located in Bradford and the west part of Leeds serving 760,000 PE. The wastewater treatment process comprises pre-treatment and primary settlement, activated sludge combined with nitrogen (N) removal via nitrification–denitrification and chemical treatment for phosphorus (P) removal (Figure 1). This process removes 97% of the total Kjeldahl nitrogen (TKN-N) and 84% of the total phosphorus (TP). Sludge from the primary and secondary treatment is stabilised in anaerobic digesters. The clarified stream produced after dewatering of the digested sludge (centrate) (Figure 1) was used to recover TP as struvite.

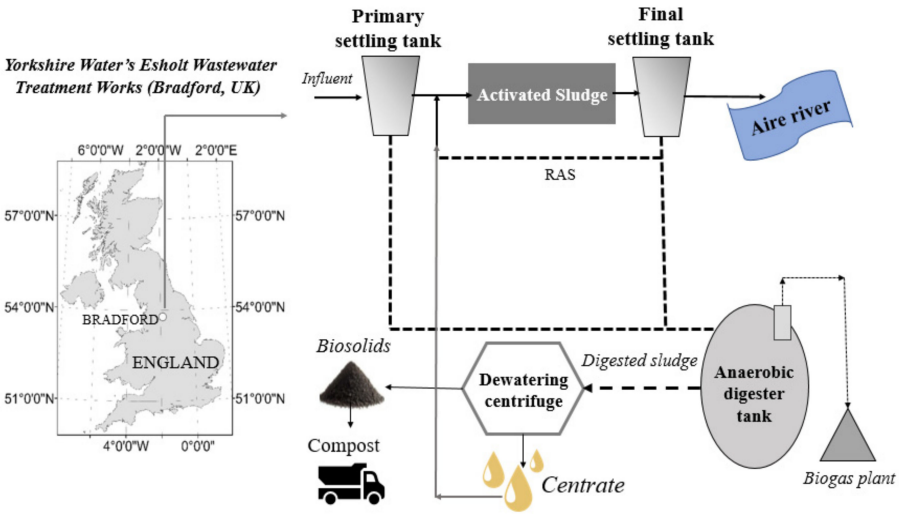

Figure 1. Esholt wastewater treatment works (Bradford, England). Data from Yulistyorini, (2016) [28].

Centrate samples were stored at 4 °C soon after sampling until used in struvite precipitation tests. This centrate has the following typical characteristics (reported as mean values): pH = 7.8; alkalinity = 4587 mg $CaCO_3$/L; ammonium = 1080 mg NH_4^+-N/L; inorganic phosphorus = 2.5 mg PO_4^{3-}-P/L; calcium = 92 mg Ca^{2+}/L; and magnesium = 32 mg Mg^{2+}/L (Table S1). Despite the absence of an enhanced biological P removal process resulting in a low P concentration, use of this centrate for the struvite precipitation tests was decided because it represents the typical complex matrix of real digested waste-activated sludge (P concentrations in the centrate were adjusted to meet typical values, see Section 2.4 and Table 1).

Table 1. Experimental conditions for pH and temperature (T) tests.

Experimental Conditions	pH-Tests	*t*-Tests
Test variables		
pH	8, 9, 10	9
Temperature (°C)	20	25, 33, 40
Stirring speed (rpm)	85	100
Velocity gradient, *G* (s^{-1})	79	79
Volume (L)	2	1
Replicates	2	2
Molar ratios		
Mg/Ca	2.3	7.1
N/P	21.6	8.6
Mg/P	1.3	1.7
Concentration of chemical species		
PO_4-P (mg/L)	120	300
NH_4-N (mg/L)	1172	1172
Mg (mg/L)	125	387
K (mg/L)	111	111
Ca (mg/L)	91.5	91.5
TSS (mg/L)	512	202

2.2. Analytical Methods

The concentration of Ca^{2+}, Mg^2 and K^+ was quantified by ionic chromatography (Metrohm 850 Professional IC with a Metrosep C4 100/4.0). The content of total suspended solids (TSS) and volatile suspended solids (VSS) in the centrate, as well as ammonium content (NH4+-N) in struvite precipitates, were determined according to Standard Methods [29]; struvite precipitates were dissolved in acid (HCl 0.1 M) before distillation for ammonium characterisation. Further analyses to determine the content of NH_4^+-N, TKN-N, TP, and PO_4^{3-}-P in the solution were conducted following standardised methodologies developed by HACH®, for use in an automated water analysis Laboratory Robot (AP3900 MULTI, Laboratory Robot, HACH): tests LCK 302 and 305 (ammonium), APC350 and APC350o (total phosphorus and orthophosphate), and APC238 (Total Kjeldahl Nitrogen).

2.3. Struvite Precipitate Characterisation

The morphology of struvite precipitates was identified by scanning electron microscopy (SEM; ZEISS EVO®LS 15, INCA analyser). The crystalline nature and the semi-quantitative composition (purity) were determined by X-ray diffraction (XRD; Bruker D2 Phaser), using struvite standard x-ray diffraction patterns (PDF number 01-071-2089 and 01-077-2303); data processing was conducted using DIFRACC SUITE EVA, High Score Plus 3.0e software and the Crystallography Open Database. Crystal size was quantified using ImageJ software [30], measuring 60 crystals per sample on average.

2.4. Materials

In all experiments, magnesium chloride hexahydrate ($MgCl_2 \cdot 6H_2O$) was added to meet a molar ratio Mg: Ca >2 and Mg: P > 1, which were selected based on data reported

by Li et al. [18] and Liu et al. [31] who found struvite crystals with high purity and high phosphorus recovery when using these molar ratios.

The concentration of PO_4^{3-}-P in centrate samples was adjusted to 120 and 300 mg P/L, using sodium dihydrogen phosphate (NaH_2PO_4) for pH and temperature (T) tests, respectively. These phosphate concentration values are within the typical range reported for real AD centrate samples from WWTWs with enhanced biological phosphorus removal (EBPR) [32–34]. The P concentration in *t*-tests (300 mg P/L) was deliberately higher than in pH-tests (120 mg P/L) to produce enough struvite precipitate for subsequent characterisation. This consideration was made because *t*-tests were carried out in smaller reactors (1 L) than those used in pH-tests (2 L). The pH of the tested centrate samples was adjusted to 8, 9 and 10 using a 1 M sodium hydroxide (NaOH) solution. All chemical reagents used were analytical grade.

2.5. Experimental Set-Up and Procedure

Experimental conditions for pH-tests and *t*-tests are reported in Table 1. The velocity gradient (*G*) was set at 79 s^{-1}, following a previous study where the largest struvite precipitate particle size was obtained when *G* values ranged between 79 and 188 s^{-1} [35]. Two tests were done: pH (pH-tests) and temperature (*t*-tests) tests, both in a standard jar tester (PB-900 Phipps & Bird) (Figure 2), with acrylic plastic jars of 2.0 L or 1 L, respectively, submerged into a water bath with temperature control. The pH-tests were conducted at a fixed temperature (20 °C) at three pH levels (8, 9 and 10). Then, *t*-tests were conducted at a fixed pH of 9 and at three temperature levels (25, 33, and 40 °C). Only in *t*-tests, the centrate was centrifuged to reduce the concentration of total suspended solids (TSS) and to obtain a struvite with fewer impurities.

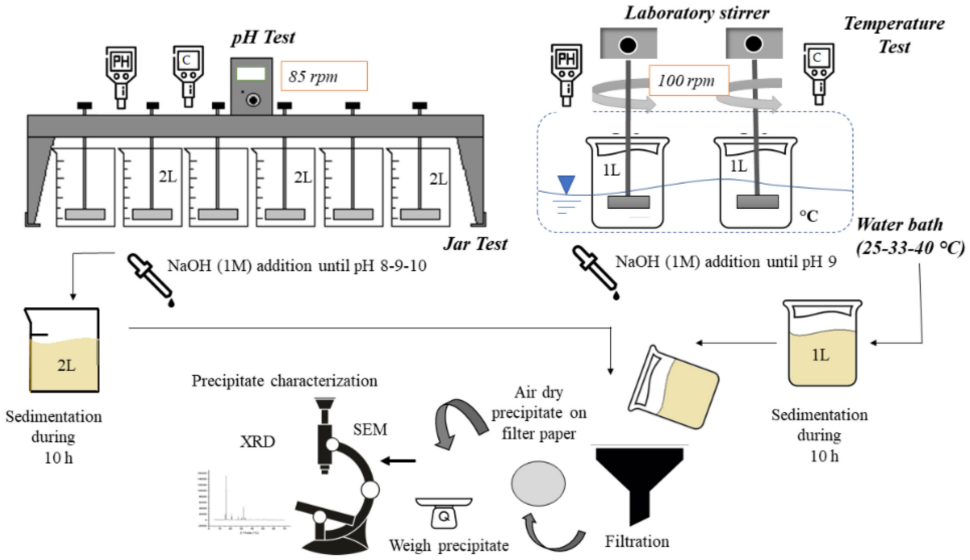

Figure 2. Experimental procedure for struvite precipitation in pH and temperature tests.

All tests were performed by duplicate over 3 h of reaction time. Although the time required to begin struvite nucleation varies between 10 and 45 min [23], a longer reaction time was chosen to form large crystals [36]. The sedimentation time was 10 h to increase particle recovery. Precipitates were separated by vacuum filtration using a 0.45 µm pore size filter (fibreglass) and air-dried at room temperature (Figure 2).

2.6. Data Processing and Statistical Analysis

ANOVA one factor analysis was performed for pH and temperature tests to assess statistically significant differences between each level of the variables tested (differences exist in at least one pair of data if $p < 0.05$).

The Thermodynamic Visual MINTEQ 3.1 software (U.S. Environmental Protection Agency) was used to calculate the SI of other compounds that can precipitate under the experimental conditions: (i) when SI = 0, the solution is in equilibrium; (ii) when SI < 0, the solution is undersaturated, and no precipitation occurs; (iii) when SI > 0, the solution is supersaturated, and precipitation occurs spontaneously. SI was calculated using Equation (1), where *IAP* is the ion activity product and K_{SP} is the solubility product constant of the selected solid substance dissolving in the aqueous solution.

$$\mathrm{SI} = \log \frac{IAP}{K_{SP}} \quad (1)$$

Visual MINTEQ version 3.1 was also used in this study to predict concentrations of species in the aqueous solution. The modelling process was based on the concentrations of chemical species reported in Table 1.

The quantity precipitated in each trial was calculated as the amount of TSS formed. Therefore, it was calculated as the final weight of the precipitate minus the initial amount of TSS in the solution. The mass balance per test was calculated on a mmol basis. The concentrations of Mg^{2+}, $PO_4{}^{3-}$-P, Ca^{2+} and K^+ precipitated were calculated based on the difference between their initial and final molar concentrations in solution. The amount of $NH_4{}^+$-N contained in the precipitates was calculated by multiplying the precipitate mass (g) by its N content (%, dry weight). An N molar mass balance was calculated in all tests to find the amount (mmol) of N volatilised (NH_3-N), according to Equation (2), where each term is reported as molar mass (mmol) [15].

$$(\mathrm{NH_3 - N})_{\mathrm{volatilized}} = (\mathrm{NH_4 - N})_{\mathrm{initial-liquid}} - (\mathrm{NH_4 - N})_{\mathrm{final\ liquid}} - (\mathrm{NH_4 - N})_{\mathrm{final\ solid}} \quad (2)$$

According to Li et al. [18], ammonia nitrogen can be used as a proxy element to calculate the struvite content in the total solid product since struvite is the only possible precipitate containing ammonia nitrogen. However, considering that struvite has an N: P: Mg molar ratio of 1: 1: 1, in this study, the number of precipitated mmoles of struvite (nMAP) in each test was assumed to be the lowest value between the precipitated mmoles of Mg^{2+}, $PO_4{}^{3-}$-P and $NH_4{}^+$-N; therefore, the quantity of ions that did not precipitate as struvite were calculated as the difference between the mmoles of MAP and the mmoles precipitated of each ion. The percentage of phosphate as struvite (P_{MAP}, %) was calculated as the ratio of nMAP (mmol) and the initial mmoles of $PO_4{}^{3-}$-P in the solution, as shown in Equation (3) [15].

$$\mathrm{P_{MAP}}(\%) = \frac{\mathrm{n\ MAP}}{(\mathrm{PO_4 - P})_{\mathrm{initial}}} \times 100 \quad (3)$$

The struvite purity was calculated as the percentage of struvite in the final solid precipitate using Equation (4), where $M_{struvite}$ is the molar mass of struvite (245 g/mol), and $m_{product}$ is the final precipitated mass (g) obtained in each test [37].

$$\mathrm{Purity}(\%) = \frac{\mathrm{n\ MAP.M_{struvite}}}{\mathrm{m_{product}}} \times 100 \quad (4)$$

3. Results and Discussion

3.1. Effect of the pH and Temperature on Ions Removal

The Mg and P removal as struvite was similar at the three pH conditions evaluated (i.e., pH 8, 9 and 10) at high concentrations (7.9 mmol; calculated from the initial mmol of P in the solution; Figure 3a). The removal of the Ca and N increased as the pH value increased (Figure 3a), explained by the formation of calcium carbonates ($CaCO_3$) and calcium phosphates ($Ca_3(PO_4)_2$). The ammonium removal can be explained as a combination of the precipitation and volatilisation processes, the latter favoured under well-mixing conditions at higher pH levels. The percentage of volatilised NH_3-N was 13, 22 and 54% of the total initial ammonium concentration for the pH values of 8, 9 and 10, respectively (Table 2).

These values agree with data from the model simulation runs using Visual MINTEQ (see Section 3.2.), which predicted an increase in NH_3(aq) with an increasing pH value (4, 30 and 76% for pH 8,9 and 10, respectively).

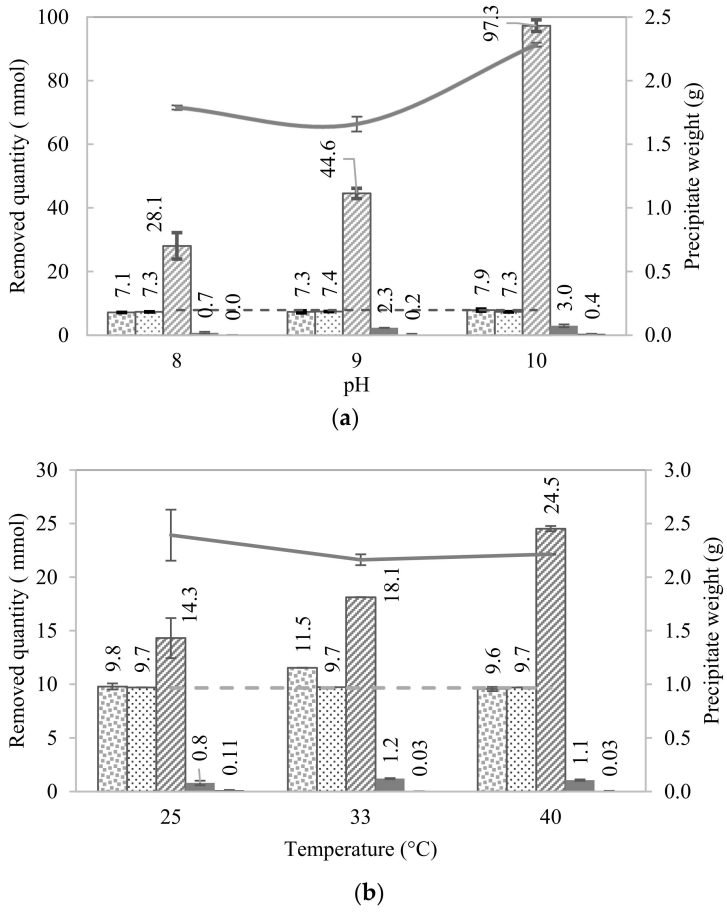

Figure 3. Removed quantities of Mg, P, N, Ca and K from the solution and recovered mass as a precipitate in pH (**a**) and *t* (**b**) tests. Symbols: Mg, P, N, Ca, K precipitate mass, maximum quantity (mmol) that can precipitate as struvite.

Table 2. Removal efficiency per ion, precipitate quality (mass and richness; particle size).

	T (°C)	20	20	20	25	33	40	ANOVA	
	pH	8	9	10	9	9	9	*p*-Value	
Parameter								pH	T
Removal efficiency * (%)	Mg^{2+}	68.6 ± 0.1	70.4 ± 3.0	75.8 ± 3.0	60.8 ± 1.5	71.6 ± 0.1	59.3 ± 1.2	0.118	0.004
	Ca^{2+}	15.9 ± 7.8	50.6 ± 0.5	64.5 ± 10.0	35.2 ± 9.1	52.7 ± 2.3	46.5 ± 2.9	0.014	0.109
	PO_4^{3-}-P	92.7 ± 0.3	93.9 ± 0.0	92.8 ± 0.4	99.5 ± 0.1	99.8 ± 0.1	99.6 ± 0.0	0.029	0.037
	NH_4^+-N	16.8 ± 2.5	26.6 ± 1.0	58.1 ± 1.1	18.6 ± 2.4	23.5 ± 0.0	31.8 ± 0.3	0.0003	0.006
	NH_3-N_{Vol}	13.1 ± 2.5	22.2 ± 1.1	53.7 ± 1.1	5.4 ± 1.2	12.8 ± 0.7	18.7 ± 0.3	0.0003	0.001
	K^+	0.7 ± 1.0	3.1 ± 4.5	7.1 ± 0.2	3.9 ± 1.5	0.9 ± 0.2	0.8 ± 1.4	0.261	0.192
MAP precipitates	P_{MAP} (%)	78.4 ± 0.5	92.7 ± 4.0	92.8 ± 0.4	99.6 ± 0.1	85 ± 1.8	98.1 ± 2.0	0.002	0.071
	Purity (%)	56	70	56	93	87	98	-	-
	Score ** (%)	55	87	68	72	66	74	-	-
	Mass (g)	1.8 ± 0.0	1.7 ± 0.1	2.3 ± 0.0	2.4 ± 0.2	2.2 ± 0.1	2.2 ± 0.0	0.001	0.359
	SI ***	1.71	2.55	2.80	3.19	3.11	3.07	-	-
	size (µm)	72 ± 30.2	84 ± 25.6	46 ± 8.7	44 ± 7.2	58 ± 15.6	52 ± 8.6	0.008	0.007

Abbreviations: P_{MAP}, percentage of phosphate as struvite; SI, saturation index; T, temperature trial; NH_3-N_{Vol}, N volatilised. Note: * Percentage of the corresponding initial soluble ion concentration. ** Score denotes similarity between X-ray diffraction profiles of pure struvite and obtained precipitates. *** SI of MAP was calculated using a mathematical model (see Figure 4).

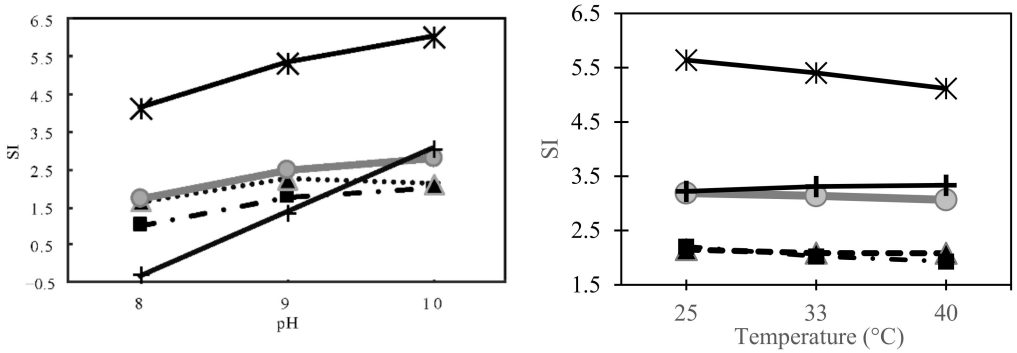

Figure 4. Saturation index (*SI*) calculated with Visual MINTEQ software for expected precipitates at (**a**) pH = 8, 9 and 10; (**b**) temperature = 25, 33 and 40 °C. Symbols: Struvite $MgNH_4PO_4.6H_2O$, Magnesite $MgCO_3$, Calcite $CaCO_3$, Farringtonite $Mg_3(PO_4)_2$, Amorphous calcium phosphate $Ca_3(PO_4)_2$.

In the pH-tests, the PO_4^{3-}-P removal efficiency was >92%, the K removal efficiency was <7% (Table 2), and the Ca precipitation was minimal in all of the experiments (Figure 3). The Mg removal efficiency was similar in all of the experiments (pH 8, 9 and 10) based on the statistical analysis of the experimental data (Anova; *p*-value = 0.11). The P_{MAP} was higher at a pH of 9 and 10 than at a pH of 8 (Table 2). The precipitates mass was higher at a pH of 10 and the purity was higher at a pH of 9, indicating that at a pH of 8 and 10, other products in addition to the struvite were possibly co-precipitated. The best relation between the P_{MAP} and purity was reached at a pH of 9, where the SI almost reached the optimum value of 2.4 for P removal [38].

In the *t*-tests, the most effective removal of Mg and Ca occurred at 33 °C (Figure 3b). This temperature also corresponds to the mean centrate temperature after the sludge dewatering and the maximum struvite solubility [26], meaning that part of the struviteprecursor ions are dissolved and available to form other salts such as farringtonite ($Mg_3(PO_4)_2$), magnesite ($MgCO_3$) or calcium phosphate ($Ca_3(PO_4)_2$). In addition, the P_{MAP} and purity decreased in comparison with the results at 25 and 40 °C.

Due to a lower TSS concentration and a higher phosphate concentration (Table 1), the purity (>87%) and phosphorus removal efficiency (>99.5%) was higher in the *t*-tests than in the pH-tests (Table 2). The NH_4^+-N removal also increased with the temperature (Table 2), with an increased NH_3-N volatilisation of 5, 12 and 17% of the total initial ammonium concentration at temperatures of 25, 33 and 40 °C, respectively. This is consistent with the model simulations using Visual MINTEQ that showed an increase in the percentage of NH_3 (aq) as the temperature rose: 30, 42 and 54% of the total initial ammonium concentration at 25, 33 and 40 °C, respectively.

3.2. Ions Mass Balance

The SI value was estimated using Visual MINTEQ 3.1 software (Figure 4). According to the current literature [16,17,20] and the molar mass balance developed in this research (Table 3), five compounds were considered as possible precipitates: (a) struvite, (b) amorphous calcium phosphate ($Ca_3(PO_4)_2$; ACP), (c) calcite ($CaCO_3$), (d) magnesite ($Mg_3(PO_4)_2$) and (e) farringtonite $Mg_3(PO_4)_2$. Amorphous calcium phosphate $Ca_3(PO_4)_2$ (ACP) and calcite $CaCO_3$ were considered as probable precipitates, but struvite kinetics formation is likely to be faster than that of the ACP. The presence of the Mg^{2+}, phosphates and dissolved organic compounds could decrease the rate of calcite precipitation. Magnesite precipitates are usually present in negligible quantities in the anaerobic digestion centrates and farringtonite $Mg_3(PO_4)_2$ can be principally formed at a higher pH value [39] (Figure 4).

Table 3. Ion balance of precipitates, including struvite and non-struvite precipitates.

Test Conditions		Quantity of Total and Individual Ions in the Precipitates (mmol)										
		Total Precipitates and MAP [1]					Non-Struvite Precipitates (See Figure 4)					
T (°C)	pH	Mg^{2+}	Ca^{2+}	NH_4^+-N	PO_4^{3-}-P	K^+	MAP [1]	Mg^{2+}	Ca^{2+}	NH_4^+-N	PO_4^{3-}-P	K^+
20	8	7.1	0.7	6.2	7.3	0.0	6.2	0.9	0.7	0.0	1.1	0.0
20	9	7.3	2.3	7.4	7.4	0.2	7.3	0.0	2.3	0.1	0.1	0.2
20	10	7.9	3.0	7.4	7.3	0.4	7.3	0.6	3.0	0.1	0.0	0.4
25	9	9.8	0.8	10.1	9.7	0.1	9.7	0.1	0.8	0.4	0.0	0.1
33	9	11.5	1.2	8.3	9.7	0.0	8.3	3.3	1.2	0.0	1.4	0.0
40	9	9.6	1.1	10.1	9.7	0.0	9.6	0.0	1.1	0.5	0.1	0.0

[1] MAP is the maximum amount of struvite (mmol) that precipitated in each test.

The low amount of removed potassium found in the experiment (<7%), indicating that potassium struvite ($MgKPO_4.6H_2O$) was not formed, can be explained by the high ammonium concentration in the experiments and the amount predicted by the model [40]. Other solids such as dolomite $CaMg(CO_3)_2$, hydroxyapatite $Ca_{10}(PO_4)_6(OH)_2$ (HA) or huntite $Mg(CaCO_3)$ were not considered as possible precipitates, based on their slow-forming kinetics [16,39] and on the duration of these tests. Newberyite $MgHPO_4{:}3H_2O$ was also not considered because it only precipitates at pH < 6 when high concentrations of magnesium and phosphorus are present [16].

Considering that struvite has a N: P: Mg molar ratio of 1: 1: 1, the maximum moles of struvite that could be precipitated in each test was quantified as the lowest value between the precipitated mmoles of Mg^{2+}, PO_4^{3-}-P and NH_4^+-N (Table 3). According to the results, the least amount of struvite and calcium phosphates appeared at a pH of 8, likely due to their higher solubility at this pH level [41]. Other Mg and P non-struvite precipitates likely formed at this pH level because of the oversaturation of the $Ca_3(PO_4)_2$ and $MgCO_3$ (Figure 4; Table 3).

The maximum amount of struvite precipitated at both a pH of 9 and a pH of 10 was 7.3 mmol; however, these conditions also precipitated the highest concentrations of Ca and Mg (Tables 2 and 3). Although the SI of $Ca_3(PO_4)_2$ increased with the pH level (Figure 4), the most feasible Ca-precipitate at a pH of 10 is $CaCO_3$ since high alkalinity levels favour its formation [42]. Additionally, at high alkalinity levels, HCO_3^- and CO_3^{2-} can bond with Mg^{2+} ions, leading to the formation of stable aqueous phases of $MgCO_3$, $Mg(HCO_3)_2$, therefore reducing the availability of this constituent for struvite nucleation [9]. Both $MgCO_3$ and $CaCO_3$ presented a high SI value at a pH of 10 (Figure 4).

In the temperature tests, the least amount of precipitated struvite and the maximum quantity of Mg, Ca and P in the non-struvite precipitates occurred at 33 °C (Table 3). According to the calculated SI values, $CaCO_3$, $Mg_3(PO_4)_2$ and $Ca_3(PO_4)_2$ can be taken as impurities in the precipitate. Regarding the NH_4^+-N removal at 25 and 40 °C, it has been reported that a small amount could be removed as NH_4OH [8] (<0.5 mmol); however, this is very unlikely. In fact, the model in Visual MINTEQ did not predict the NH_4^+-N precipitates other than the struvite, in agreement with the findings of Li et al. [43].

3.3. Struvite Characterisation

In all tests, the MAP precipitation was favoured compared to the other Mg and Ca precipitates confirmed by the XRD analysis (Figure 5). Results from the High Score Plus software used to process the XRD data and the corresponding scores were calculated for all the precipitates, determining how well their XRD profiles matched with the struvite standards, where a higher score indicates a better match. According to the results, a maximum score of 87% was found at a pH of 9. The peaks in the diffraction patterns could be assigned to the struvite in all sets of conditions between pH 8 and 10, increasing progressively in crystallinity (Figure 5; Table 2). No other crystalline phases were identified, demonstrating that the precipitates consist in struvite. In the *t*-tests, the diffraction patterns

from the solids of the experiments at 25 °C, 33 °C and 40 °C also showed the presence of struvite, but in a lower degree of crystallinity compared to that of the test at a pH of 10.

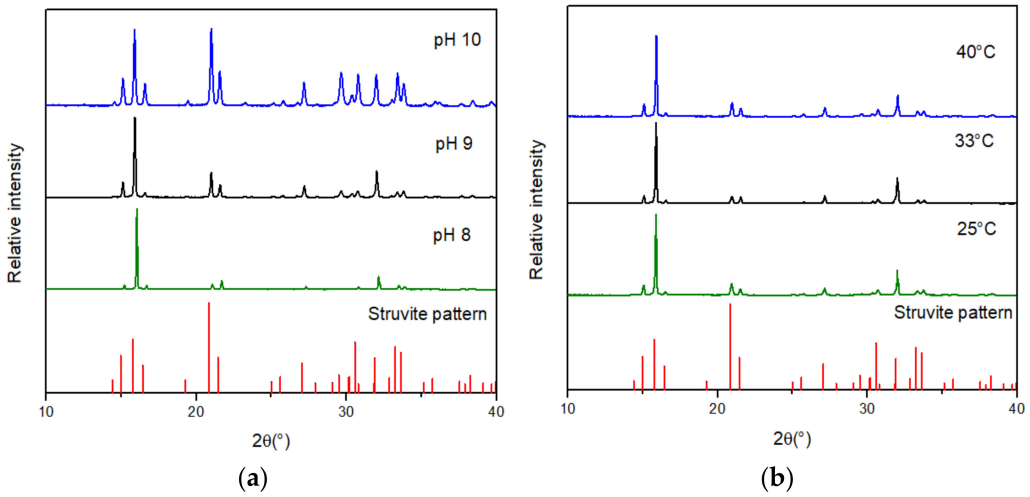

Figure 5. X-ray diffraction (XRD) diagram of precipitates obtained in the pH (**a**) and temperature (**b**) tests.

The purity of the final product is essential for the successful and economic recovery of the MAP crystals; a high product purity would improve both the product's effectiveness for end-use application and the market price. The high TSS content of centrates and the moderate concentration of ions in the solution, such as Ca^{2+}, K^{+} and CO_3^{2-}, could affect the purity of the formed struvite [20,44]. However, the high N:P molar ratio of the centrate and the molar ratios of the Mg:Ca > 2 and Mg: P > 1 improved the precipitation of struvite over other precipitates such as calcium and magnesium phosphate [15].

The product quality also includes the struvite morphology and particle size distribution, as these are all relevant characteristics for the end-use product. Particle size is an essential characteristic during crystallisation. Larger particle sizes of struvite are of particular interest for applications as fertiliser since the MAP released from this mineral is slow because of the lower surface area to volume ratio [18]. In the pH-tests, the largest mean particle size was obtained at a pH of 8 (72 µm) and a pH of 9 (84 µm), meanwhile the largest mean particle size was obtained at 33 °C (58 µm) in the *t*-tests (Figures 6 and S1, and Table 2). An increase in the saturation ratio increases the nominal weight of the fines since a higher SI level results in a higher nucleation rate than the crystal growth rate [38]. Therefore, due to the higher struvite SI at a pH of 10 (2.8) and temperature of 25 °C (3.19), the mean particle size was smaller in these two tests (Figure 6c,d). Although the SI is lower at a pH of 8 than at a pH of 9, the particle size did not show significant differences (ANOVA; *p*-value > 0.05), possibly because the reaction rates are lower at a pH of 8, and the reaction time was not enough to obtain the maximum particle size.

All the obtained particle sizes were smaller than those sizes previously reported to facilitate a low release of P and N in crops (>1 mm) [6]. This may be related to the presence of Ca, the high SI produced by the high concentration of ammonium in the centrate and the low reaction time in the tests (3 h) [27,45,46].

In the crystallisation process, the settling velocity is an essential factor in ensuring efficient solid–liquid separation and obtaining a more significant recovery of nutrients. The settling velocity is strongly dependent on the sizes and morphology of the precipitates. According to Shaddel et al. [27], the bigger crystals settle faster for all the morphologies; additionally, among different morphologies, the bipyramidal crystals have the highest settling velocity for all crystal sizes, followed by the X-shape and the dendritic crystals.

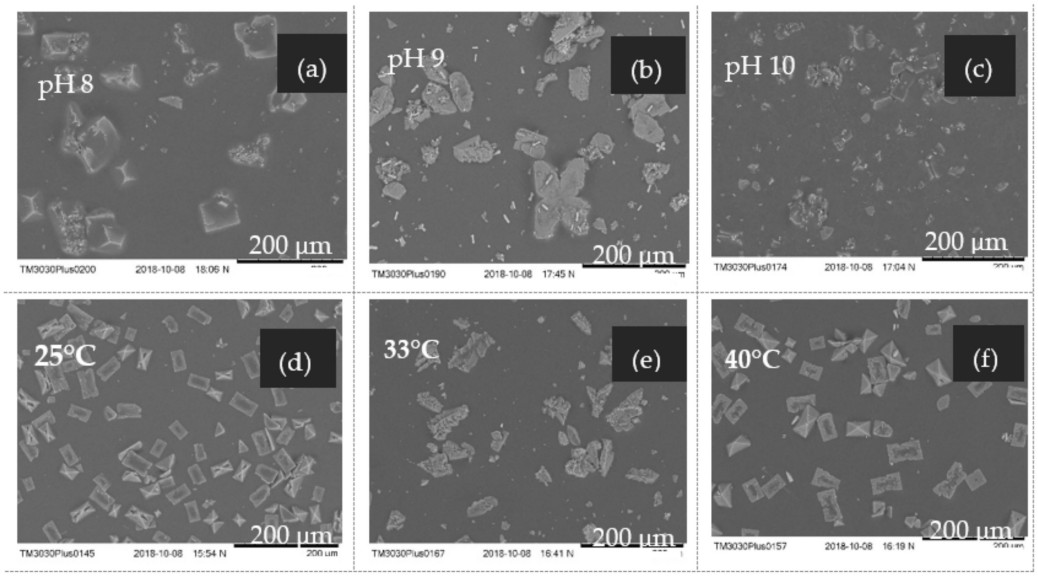

Figure 6. SEM images of precipitates obtained in pH-tests at T = 20 °C (**a**–**c**) and temperature tests at pH 9 (**d**–**f**) trials.

A plate crystal morphology enhanced with a low SI (1.56) was predominantly formed at a pH of 8, in comparison to that formed at a pH of 9 and10. A more dendritic crystal with a less defined X-shape morphology was obtained at a pH of 10, exhibiting particle agglomeration that can be explained by the high SI at this pH condition [27,38].

The struvite morphologies obtained in this work at 25 and 40 °C showed a well-faceted structure with a bipyramidal appearance, while at 33 °C a combination of different morphologies were obtained, likely due to the presence of Ca and Mg in the system.

Another important factoraffecting the crystal size and shape is the N:P molar ratio; higher relations increase the crystal size and change the crystal shape from a triangular prism to an irregular X shape [4].

In this work, the best-operating conditions to obtain pure struvite crystals with a higher sedimentation rate were at a pH of 9 (high N:P molar ratio, 21.6:1) and a temperature of 40 °C because under these conditions, the largest particle sizes and the highest material purity were obtained.

4. Conclusions

The research reported in this paper provides a systematic methodology that can be used to optimise the process conditions to enhance both the quality and quantity of struvite precipitates, as a strategy to recover nutrients (nitrogen and phosphorus) from real AD centrates with high ammonium and phosphate concentrations.

The influence of the pH and temperature on struvite precipitation (MAP removal) efficiency and purity from a real complex centrate, from the dewatering of digested municipal sludge, was investigated. In all the conditions tested, P-removal was favourable with an efficiency higher than 93%; however, to obtain struvite with a higher purity and a larger particle size (allowing for a slower release of nutrients in its application as a fertiliser) the suggested conditions are a pH of 9 and a temperature of 40 °C, linked to a system where any ammonium lost due to volatilisation is also recovered (i.e., acid solution absorption) to avoid its release into the environment.

The purity of the struvite was influenced by the presence of Mg^{2+}, Ca^{2+}, PO_4^{3-} and the TSS content of the initial centrate, as well as by the pH level and temperature. Although the high concentration of ammoniacal N in the centrate favours the purity of the struvite obtained, such purity was strongly reduced at a pH of 8 and 10, and at a temperature of 33 °C. A pH of 8 could favour the precipitation of Ca and Mg compounds, such as

$Ca_3(PO_4)_2$ and $MgCO_3$, whereas the most feasible Ca-precipitate is $CaCO_3$ at a pH of 10, since high alkalinity levels favour its formation.

The temperature of 33 °C, which is typical of sludge dewatering supernatants (by centrifuge), is not recommended to precipitate struvite, since the solubility of the struvite is at its maximum at this temperature and therefore, the precipitation of other compounds such as $CaCO_3$, $Mg_3(PO_4)_2$ and $Ca_3(PO_4)_2$ is favoured.

Under more practical conditions, the recommended process conditions for P recovery as struvite precipitates from the digester supernatant (centrate) from a WWTW are a pH of 9 and a temperature between 20 and 25 °C. This is mainly based on the high P recovery as MAP, the purity of the crystals (70–93%), the lower precipitation of impurities and the acceptable ammonia loses due to volatilisation at lower temperatures.

Supplementary Materials: The following are available online at https://www.mdpi.com/article/10.3390/su131910730/s1, Table S1: Characteristics of digested sludge supernatant (centrate) sampled from Esholt WWTW. Figure S1: Particle size in (a) pH-tests; (b) *t*-tests.

Author Contributions: Conceptualization, C.G.-M. and M.A.C.-V.; methodology, M.A.C.-V., B.F. and C.G.-M.; formal analysis, C.G.-M., D.N.-F. and A.M.-V.; investigation, C.G.-M.; resources, M.A.C.-V. and B.F.; writing—original draft preparation, C.G.-M.; writing—review and editing, B.F., C.G.-M., D.N.-F., A.M.-V., M.A.C.-V. and F.J.M., supervision, M.A.C.-V. and F.J.M.; project administration, F.J.M.; funding acquisition, F.J.M., M.A.C.-V. and B.F. All authors have read and agreed to the published version of the manuscript.

Funding: C. González thanks Minciencias and Enlaza Mundos for the financial support of her PhD Internship. IRTA thanks the financial support of the CERCA program of the Generalitat de Catalunya government and the National Institute of Agronomic Research (INIA) of the Ministry of Science and Innovation—Spanish government through the research project PIONER (ref. RTA2015-00093-00-00).

Data Availability Statement: Not applicable.

Acknowledgments: The authors thank David Elliot, Lucy Leonard and Christian Aragon from the School of Civil Engineering, University of Leeds; Celia Segura and Marlene Mendoza from IRTA; and GAIA group from Universidad de Antioquia for their technical support, as well as Yorkshire Water's Esholt WWTW for facilitating the sample collection.

Conflicts of Interest: The authors declare no conflict of interest.

References

1. Li, B.; Boiarkina, I.; Young, B.; Yu, W.; Singhal, N. Prediction of Future Phosphate Rock: A Demand Based Model. *J. Environ. Inform.* **2018**, *31*, 4153. [CrossRef]
2. Ungureanu, N.; Vlăduț, V.; Voicu, G. Water scarcity and wastewater reuse in crop irrigation. *Sustainability* **2020**, *12*, 119. [CrossRef]
3. Adegoke, A.A.; Amoah, I.D.; Stenström, T.A.; Verbyla, M.E.; Mihelcic, J.R. Epidemiological evidence and health risks associated with agricultural reuse of partially treated and untreated wastewater: A review. *Front. Public Health* **2018**, *6*, 1–20. [CrossRef]
4. Liu, Y.; Qu, H. Interplay of digester supernatant composition and operating pH on impacting the struvite particulate properties. *J. Environ. Chem. Eng.* **2017**, *5*, 39493955. [CrossRef]
5. Guadie, A.; Xia, S.; Jiang, W.; Zhou, L.; Zhang, Z.; Hermanowicz, S.W.; Shen, S. Enhanced struvite recovery from wastewater using a novel cone-inserted fluidized bed reactor. *J. Environ. Sci.* **2014**, *26*, 765774. [CrossRef]
6. Rahman, M.M.; Salleh, M.A.M.; Rashid, U.; Ahsan, A.; Hossain, M.M.; Ra, C.S. Production of slow release crystal fertilizer from wastewaters through struvite crystallization-A review. *Arab. J. Chem.* **2013**, *7*, 139155. [CrossRef]
7. Batstone, D.J.; Jensen, P.D. Anaerobic Processes. *Treatise Water Sci.* **2011**, *4*, 615639.
8. Tansel, B.; Griffin, L.; Monje, O. Struvite formation and decomposition characteristics for ammonia and phosphorus recovery: A review of magnesium-ammonia- phosphate interactions. *Chemosphere* **2018**, *194*, 504514. [CrossRef] [PubMed]
9. Siciliano, A.; Limonti, C.; Curcio, G.M.; Molinari, R. Advances in struvite precipitation technologies for nutrients removal and recovery from aqueous waste and wastewater. *Sustainability* **2020**, *12*, 7538. [CrossRef]
10. Snoeyink, V.; Jenkins, D. *Water Chemistry*; John Wiley and Sons: New York, NY, USA, 1980.
11. Doyle, J.D.; Philp, R.; Churchley, J.; Parsons, S.A. Analysis of Struvite Precipitation in Real and Synthetic Liquors. *Process. Saf. Environ. Prot.* **2000**, *78 Pt B*, 480–488. [CrossRef]
12. Le Corre, K.S.; Valsami-Jones, E.; Hobbs, P.; Parsons, S.A. Phosphorus recovery from wastewater by struvite crystallization: A review. *Crit. Rev. Environ. Sci. Technol.* **2009**, *39*, 433477. [CrossRef]

13. Shih, K.; Yan, H. Chapter 26—The Crystallization of Struvite and Its Analog K-Struvite From Waste Streams for Nutrient Recycling. In *Environmental Materials and Waste*; Prasad, M.N., Shih, K., Eds.; Elsevier: Amsterdam, The Netherlands, 2016; pp. 665–686.
14. Le Corre, K.S.; Valsami-Jones, E.; Hobbs, P.; Parsons, S.A. Impact of calcium on struvite crystal size, shape and purity. *J. Cryst. Growth* **2005**, *283*, 514522. [CrossRef]
15. Capdevielle, A.; Sýkorová, E.; Biscans, B.; Béline, F.; Daumer, M.L. Optimization of struvite precipitation in synthetic biologically treated swine wastewater-Determination of the optimal process parameters. *J. Hazard. Mater.* **2013**, *244–245*, 357369. [CrossRef]
16. Hallas, J.F.; Mackowiak, C.L.; Wilkie, A.C.; Harris, W.G. Struvite Phosphorus Recovery from Aerobically Digested Municipal Wastewater. *Sustainability* **2019**, *11*, 376. [CrossRef]
17. Lee, S.H.; Yoo, B.H.; Kim, S.K.; Lim, S.J.; Kim, J.Y.; Kim, T.H. Enhancement of struvite purity by re-dissolution of calcium ions in synthetic wastewaters. *J. Hazard. Mater.* **2013**, *261*, 2937. [CrossRef]
18. Li, B.; Boiarkina, I.; Young, B.; Yu, W. Quantification and mitigation of the negative impact of calcium on struvite purity. *Adv. Powder Technol.* **2016**, *27*, 23542362. [CrossRef]
19. Moulessehoul, A.; Gallart-Mateu, D.; Harrache, D.; Djaroud, S.; de la Guardia, M.; Kameche, M. Conductimetric study of struvite crystallization in water as a function of pH. *J. Cryst. Growth* **2017**, *471*, 4252. [CrossRef]
20. Li, B.; Boiarkina, I.; Yu, W.; Huang, H.M.; Munir, T.; Wang, G.Q.; Young, B.R. Phosphorous recovery through struvite crystallization: Challenges for future design. *Sci. Total Environ.* **2019**, *648*, 12441256. [CrossRef] [PubMed]
21. Ariyanto, E.; Ang, H.M.; Sen, T.K. The Influence of Various Process Parameters on Dissolution Kinetics and Mechanism of Struvite Seed Crystals. *J. Inst. Eng. Ser. A* **2017**, *98*, 293302. [CrossRef]
22. Moussa, S.B.; Tlili, M.M.; Batis, N.; Amor, M.B. Influence of temperature on struvite precipitation by CO_2-deagassing method. *Cryst. Res. Technol.* **2011**, *260*, 255260.
23. Crutchik, D.; Garrido, J.M. Kinetics of the reversible reaction of struvite crystallisation. *Chemosphere* **2016**, *154*, 567572. [CrossRef]
24. Doyle, J.D.; Parsons, S.A. Struvite formation, control and recovery. *Water Res.* **2002**, *36*, 39253940. [CrossRef]
25. Webb, K.M.; Ho, G.E. Solubility and its application to a piggery effluent problem. *Water Sci. Technol.* **1992**, *26*, 22292232. [CrossRef]
26. Bhuiyan, M.I.H.; Mavinic, D.S.; Beckie, R.D. A solubility and thermodynamic study of struvite. *Environ. Technol.* **2007**, *28*, 10151026. [CrossRef]
27. Shaddel, S.; Ucar, S.; Andreassen, J.; Østerhus, S.W. Engineering of struvite crystals by regulating supersaturation-Correlation with phosphorus recovery, crystal morphology and process efficiency. *J. Environ. Chem. Eng.* **2019**, *7*, 102918. [CrossRef]
28. Yulistyorini, A. *Phosphorus Recovery from Wastewater through Enhanced Micro-Algal Uptake*; The University of Leeds: Leeds, UK, 2016.
29. APHA; AWWA; WEF. *Standard Methods for the Examination of Water and Wastewater*, 23rd ed.; American Public Health Association: Washington, DC, USA, 2017.
30. Rasban, W. Image J. National Institutes of Health. 2016. Available online: https://imagej.nih.gov/ij/download.html (accessed on 1 July 2021).
31. Liu, Z.; Zhao, Q.; Lee, D.; Yang, N. Enhancing phosphorus recovery by a new internal recycle seeding MAP reactor. *Bioresour. Technol.* **2008**, *99*, 64886493. [CrossRef]
32. Cabanelas IT, D.; Ruiz, J.; Arbib, Z.; Chinalia, F.A.; Garrido-Pérez, C.; Rogalla, F.; Perales, J.A. Comparing the use of different domestic wastewaters for coupling microalgal production and nutrient removal. *Bioresour. Technol.* **2013**, *131*, 429436. [CrossRef]
33. Munch, E.V.; Barr, K. Controlled Struvite Crystallisation for Removing Phosphorus From Anaerobic Digestion Sidestreams. *Water Res.* **2001**, *35*, 151159. [CrossRef]
34. Jia, G. *Nutrient Removal and Recovery by the Precipitation of Magnesium Ammonium Phosphate*; The University of Adelaide: Adelaide, SA, Australia, 2014.
35. González-Morales, C.; Camargo-Valero, M.A.; Molina-Pérez, F.J.; Fernandez, B. Effect of the stirring speed on the struvite formation using the centrate from a WWTP. *Rev. Fac. Ing.* **2019**, *92*, 917. [CrossRef]
36. Liu, X.; Wen, G.; Hu, Z.; Wang, J. Coupling effects of pH and Mg/P ratio on P recovery from anaerobic digester supernatant by struvite formation. *J. Clean. Prod.* **2018**, *198*, 633641. [CrossRef]
37. Ye, X.; Ye, Z.L.; Lou, Y.; Pan, S.; Wang, X.; Wang, M.K.; Chen, S. A comprehensive understanding of saturation index and up fl ow velocity in a pilot-scale fl uidized bed reactor for struvite recovery from swine wastewater. *Powder Technol.* **2016**, *295*, 1626. [CrossRef]
38. Ghosh, S.; Lobanov, S.; Lo, V.K. Impact of supersaturation ratio on phosphorus recovery from synthetic anaerobic digester supernatant through a struvite crystallization fluidized bed reactor. *Environ. Technol.* **2019**, *40*, 2000–2010. [CrossRef]
39. Çelen, I.; Buchanan, J.R.; Burns, R.T.; Robinson, R.B.; Raman, D.R. Using a chemical equilibrium model to predict amendments required to precipitate phosphorus as struvite in liquid swine manure. *Water Res.* **2007**, *41*, 16891696. [CrossRef] [PubMed]
40. Uysal, A.; Kuru, B. Examination of Nutrient Removal from Anaerobic Effluent of the Dairy Processing Industry by Struvite Precipitation Using the Response Surface Methodology. *Fresenius Environ. Bull.* **2013**, *22*, 13801387.
41. Yan, H.; Shih, K. Effects of calcium and ferric ions on struvite precipitation: A new assessment based on quantitative X-ray diffraction analysis. *Water Res.* **2016**, *95*, 310318. [CrossRef] [PubMed]
42. Vasconcelos, C. *Estudio de la Cristalización y Recuperación de Hidroxiapatita en un Reactor de Tanque Agitado*; Universitat Politècnica de Catalunya: Barcelona, Spain, 2013.

43. Li, B.; Huang, H.M.; Boiarkina, I.; Yu, W.; Huang, Y.F.; Wang, G.Q.; Young, B.R. Phosphorus recovery through struvite crystallisation: Recent developments in the understanding of operational factors. *J. Environ. Manag.* **2019**, *248*, 109254. [CrossRef] [PubMed]
44. Zhang, D.M.; Chen, Y.X.; Jilani, G.; Wu, W.X.; Liu, W.L.; Han, Z.Y. Optimization of struvite crystallization protocol for pretreating the swine wastewater and its impact on subsequent anaerobic biodegradation of pollutants. *Bioresour. Technol.* **2012**, *116*, 386395. [CrossRef] [PubMed]
45. Stratful, I.; Scrimshaw, M.D.; Lester, J.N. Conditions influencing the precipitation of magnesium ammonium phosphate. *Water Res.* **2001**, *35*, 41914199. [CrossRef]
46. Tarragó, E.; Puig, S.; Ruscalleda, M.; Balaguer, M.D.; Colprim, J. Controlling struvite particles' size using the up-flow velocity. *Chem. Eng. J.* **2016**, *302*, 819827. [CrossRef]